RSC Advances

PAPER

Cite this: *RSC Adv.*, 2016, **6**, 20551

Effect of the alloying element on the temperature-dependent ideal shear strength of γ'-Ni_3Al

Xiaoxia Wu[ab] and Chongyu Wang*[ac]

The temperature-dependent ideal shear strength (τ_{IS}) of γ'-Ni_3Al and the effects of alloying (Re, Ru, Mo, Cr, Co, W, and Ta) were studied in terms of first-principles calculations within the {111} slip plane along the [11−2] and [−110] directions. Based on the predicted volume *versus* temperature relations, the temperature dependence of τ_{IS} was obtained using the quasistatic approach, where it was found that τ_{IS} gradually decreased with increasing temperature. For the {111}[11−2] slip systems, all of the alloying elements except for Co were found to improve the τ_{IS} of γ'-Ni_3Al at the considered temperature. Among these elements, Re was the most effective element, and doping a small amount of Re (~3 at%) was found to increase τ_{IS} by ~23.5% at 0 K. Next, W and Mo increased the τ_{IS} by 20.2 and 18.1%, respectively. For the {111}[−110] slip systems, only Re increased the τ_{IS} of γ'-Ni_3Al while the other dopants decreased the ideal shear strength of the system at 0 K. Interestingly, a high-temperature relative strengthening *via* W alloying was observed for the γ'-Ni_3Al phase within the {111}[−110] slip system at temperatures T > 800 K. However, the sequence of the τ_{IS} of the γ'-Ni_3Al phase doped with other alloying elements was not altered by increasing temperature. According to these calculations, Re and W at the Al sites can effectively improve the shear resistance of the γ'-Ni_3Al phase, and especially at high temperature. Furthermore, the effect of alloying upon the shear strength is understood by the electronic structure analysis.

Received 15th November 2015
Accepted 14th February 2016

DOI: 10.1039/c5ra24108a

www.rsc.org/advances

1. Introduction

The Ni-based single crystal superalloy composed of the γ-Ni matrix and the γ'-Ni_3Al precipitate phases is an ideal structural material at high operating temperatures and its stability is very important for material applications.[1–3] The ideal shear strength (ISS, τ_{IS}) is the minimum stress needed to plastically deform a perfect crystal, and can be used to characterize the stability of the material. The ISS is related to the stress necessary for the nucleation of a dislocation and the formation of a stacking fault.[4] The γ'-Ni_3Al, with its anomalous temperature dependence of the yield stress,[5] is largely responsible for the strength of superalloys and their resistance to deformation at high temperatures. Therefore, a study of the mechanical behaviors of the γ' phase should partially reflect the global properties of Ni-based superalloys. With the addition of platinum metals and refractory elements such as Co, Cr, Mo, Re, Ru, Ta and W, the overall performances of superalloys have largely been improved, and especially the high-temperature creep rupture strength, thermal fatigue resistance, and oxidation resistance.[1] Also, according to recent experiments and density functional theory calculations,[6–8] alloying elements in γ'-Ni_3Al mainly occupy the Al site, so an investigation into the shear behaviors of Ni_3Al, and especially the effect of alloying, is very necessary.

Measuring the ideal strength of a material is difficult using experimental tools, and there are only a few cases of experimental data obtained from well-controlled nanoindentation experiments, including the nanoindentation result for fcc Ni measured by Lorenz *et al.*[9] and the tensile test for whiskers.[10] Because of the rapid progress of the modern computer, theoretical investigations into the ideal strength of various materials have been carried out by the first-principles method[11–16] and, so far, the theoretical tensile and shear strength of metals (Mo, W, Fe, Al, Cu, and Ni)[11–14] and the $L1_2$ intermetallic compounds (Ni_3Al, and $Co_3(Al, W)$)[15,16] have been reported. Furthermore, calculations of the ideal strength can be extended to defective systems containing a point defect,[15] an interface or a grain boundary.[17–19] For example, Wang *et al.*[15] have studied the influence of the alloying element Re upon the ideal tensile and shear strength of γ'-Ni_3Al. However, most of the calculated results have been performed at 0 K, though the temperature effect has an important influence upon the material properties. Recently, Iskandarov *et al.* have performed molecular dynamics simulations to estimate the temperature effect upon the ideal shear strength of Al and Cu,[20] while Zhou *et al.* have calculated the ideal strength of Al at finite temperatures by an *ab initio*

[a]*Central Iron and Steel Research Institute, Beijing 100081, China. E-mail: cywang@mail.tsinghua.edu.cn*

[b]*School of Mathematics, Physics and Biological Engineering, Inner Mongolia University of Science and Technology, Baotou 041010, China*

[c]*Department of Physics, Tsinghua University, Beijing 100084, China*

molecular dynamics method.[21] Also, using the first-principles method combined with a quasistatic approach, Shang *et al.* have studied the temperature-dependent ideal shear deformation of Ni.[22] However, studies focused on the temperature dependence of the $\tau_{IS,}$ of γ'-Ni_3Al is lacking, and with alloying in particular, both experimentally and theoretically.

In the present work, we mainly investigate the temperature-dependent τ_{IS} of γ'-Ni_3Al using the first-principles method, and especially the effects of alloying elements at finite temperatures. The first-principles method is based on a combination of the quasi-harmonic approximation[23,24] and the quasi-static approach[25,26] recently proposed for elastic properties, where the main input is the volume–temperature relation. The paper is organized as follows: in Section 2, we describe the methodology for calculating the shear deformation at finite temperatures. In Section 3, the calculated results at the finite temperature and analysis of the electronic structures are presented. Finally, a summary of the present work is given in Section 4.

2. Computational methodology

To estimate the finite-temperature thermodynamic properties of γ'-Ni_3Al, the Helmholtz free energy $F(V,T)$ at constant volume V and temperature T were calculated by the quasi-harmonic approximation first-principles approach[25,27] with the formalism

$$F(V,T) = E_0(V) + F_{el}(V,T) + F_{vib}(V,T), \quad (1)$$

where $F_{el}(V,T)$ is the thermal electronic contribution to the Helmholtz free energy, which is very important for metal because of the non-zero electronic density at the Fermi level. The F_{vib} parameter is the vibrational free energy of the lattice atoms described in the present work by phonon calculations, and $E_0(V)$ is the static energy at 0 K from the first-principles calculation. Using eqn (1), the Helmholtz free energies were calculated at 11 volume points every 50 K from 0 to 1600 K, which is close to the melting point of pure Ni_3Al (1663 K), and fitted to the Murnaghan equation of state[28] to determine the equilibrium volume (V_0) and bulk modulus (B_T) at finite temperatures.

Subsequently, based on the predicted relation of equilibrium volume *versus* temperature ($V_0(T)$) of the γ'-Ni_3Al with the alloying elements, we adopted a quasistatic approach recently proposed[25] to predict the temperature-dependent ISS, $\tau_{IS}(T)$. Here, we assumed that the temperature dependence of the ideal shear strength was mainly caused by volume expansion, while anharmonic effects, kinetic energy contributions and fluctuation of the microscopic stress tensors were not considered. In the present work, the shear deformation of the close-packed {111} plane along the [11−2] and [−110] directions of γ'-Ni_3Al were studied, and the deformed lattice vector $\bar{\mathbf{R}}$ was obtained using[29]

$$\bar{\mathbf{R}} = \mathbf{RD}, \quad (2)$$

where the matrix $\mathbf{R}$ represents the un-deformed lattice vectors, and the deformation matrix $\mathbf{D}$ is given as

$$\mathbf{D}_{[11-2]} = \begin{bmatrix} 1 & 0 & 0 \\ 0 & 1 & 0 \\ \gamma & 0 & 1 \end{bmatrix}, \quad \mathbf{D}_{[-110]} = \begin{bmatrix} 1 & 0 & 0 \\ 0 & 1 & 0 \\ 0 & \gamma & 1 \end{bmatrix}, \quad (3)$$

where γ is the shear strain. In this way, the shear strengths of the {111}[11−2] and {111}[−110] slip systems were calculated. The approach described in ref. 12 was adopted to calculate the shear strength at the constant volume V and temperature T. The stress–strain curves were simulated by incrementally deforming the supercell in the imposed strain direction, while all of the internal freedoms of the atom were relaxed at each step.

In this research, 32-atom 2 × 2 × 2 supercells were used for Ni_3Al with a single alloying atom X occupying the Al site in the supercell; *e.g.*, the model for $Ni_{24}Al_7X$ (X = Re, Ru, Ta, W, Mo, Cr, and Co), as shown in Fig. 1, according to the results of previous first-principles and experimental site-preference studies.[6–8] Usually, Co could occupy on Ni and Al site randomly,[8] here we just considered the case of Co at Al site for the ease of comparison. The magnetic contribution is ignored for γ'-Ni_3Al because Ni_3Al is a weak itinerant ferromagnet with a Curie temperature T_C of ∼41 K and a magnetic moment of ∼0.23 μ_B.[30] For Co doped alloys, the magnetic effect is still ignored since the small concentration of Co atom.

The total energy calculation was performed by the projector augmented wave method[31,32] implemented in VASP code,[33] while the generalized gradient approximation of Perdew *et al.*[34] was used to describe the exchange-correlation effect. Following the Monkhorst–Pack scheme,[35] a 6 × 6 × 6 k-point mesh was chosen, and to ensure convergence of the calculations, a plane-wave cutoff energy of 500 eV and an energy convergence criterion of 10^{-7} eV were used for all of the calculations for self-consistency. The atomic arrangements were relaxed using the Methfessel–Paxton method with a smearing width of 0.075 eV.[36] All atomic positions in the supercell were relaxed to equilibrium until the quantum-mechanical Hellmann–Feynman forces were less than 10^{-3} eV per Å per atom.

For the calculation of the volume *versus* temperature relation ($V(T)$), the energetic calculations were implemented by the VASP code[33] and the thermal electronic contribution were calculated within the one-electron and temperature-independent band approximations by the felec code in ATAT code,[37] while the phonon calculations were performed by the supercell method

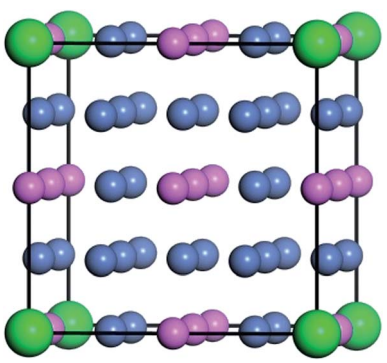

Fig. 1 The doped $L1_2$-$Ni_{24}Al_7X$ model. The blue, pink and green atoms are Ni, Al and X (X = Cr, Co, Ru, Re, Mo, W, and Ta), respectively.

with the force constants predicted by VASP code and the phonon properties were calculated by phonopy code.[38] For computational details, please refer to ref. 27. For the shear deformation along the [11−2] and [−110] direction within the {111} slip plane, the change of the shear strain γ is [0, 0.28] and [0, 0.38], respectively, with a step of 0.02.

3. Results and discussion

3.1 The temperature-dependence of the ideal shear strength

First, the stress–strain relationships of the γ'-Ni_3Al doped with the alloying elements X (X = Re, Ru, Ta, W, Mo, Cr, and Co) are performed for the {111}[11−2] and {111}[−110] slip systems at 0 K, and are plotted in Fig. 2(a) and (b), respectively. It can be seen that the calculated stress–strain curves are continuous, which demonstrates the continuity of the strain path and the reliability of the current method. From the stress–strain relationships in Fig. 2(a), the stress of the pure Ni_3Al for the {111}[11−2] slip systems increases until it reaches a maximum value of 5.768 GPa at the strain of 0.18, after which it decreases. That is to say, the ideal shear strength (ISS, τ_{IS}) of the {111}[11−2] slip system is 5.768 GPa and the corresponding critical shear strain, γ_c, is 0.18. Correspondingly, the stress of the {111}[−110] slip system reaches its maximum value, namely the ISS, of 13.710 GPa at the critical strain γ_c = 0.30, as found from Fig. 2(b). These results are in good agreement with the previous studies.[15,16] It is also found from Fig. 2(a) that all of the alloying elements except Co substantially increase the ISS value of the γ'-Ni_3Al phase under the {111}[11−2] slip systems, and Table 1 lists the values of the ISS (γ_c) and the critical strain (γ_c) for the different systems under the two slip systems. Among these elements, Re is found to be the most effective at increasing the ISS, where a relatively small doping amount of Re (~3 at%) can increase the τ_{IS} by ~23.5% at 0 K. Next, W and Mo are also effective elements, increasing the τ_{IS} by 20.2 and 18.1%, respectively. The addition of the other refractory elements Cr, Ta, and Ru also considerably increase the τ_{IS} of the γ'-Ni_3Al phases. Therefore, Re, W and Mo are the important elements for strengthening the Ni-based superalloy against shear deformation, which is the consistent with the previous prediction.[1] It is

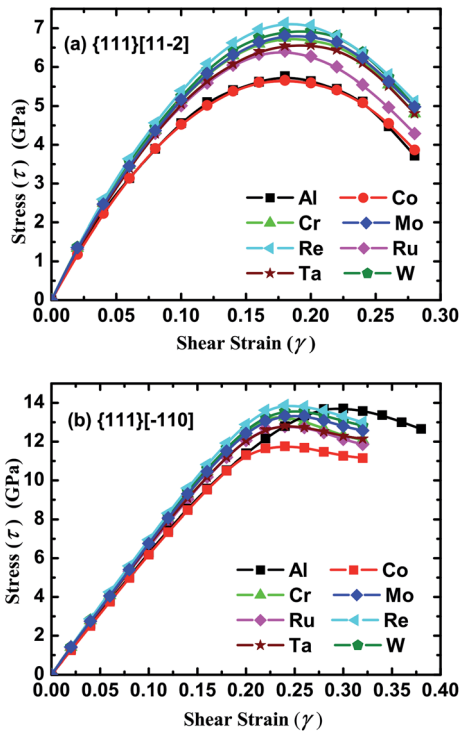

Fig. 2 Stress–strain relationships of the γ'-Ni_3Al phase doped with the different alloying elements at 0 K: (a) {111}[11−2] and (b) {111}[−110].

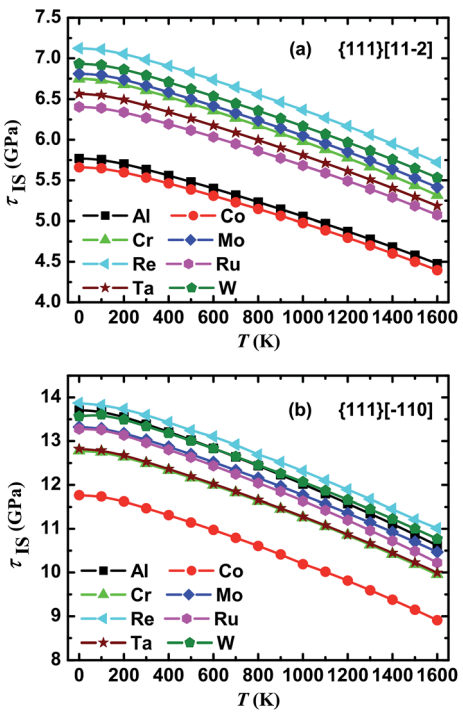

Fig. 3 The ISS of the γ'-Ni_3Al phase with different alloying elements as a function of temperature for the (a) {111}[11−2] and (b) {111}[−110] slip systems.

Table 1 The ISS (τ_{IS}) in GPa and the critical strain (γ_c) of the undoped and doped γ'-Ni_3Al phase for the two slip systems at 0 K pink

Slip system		Undoped	Co	Cr	Mo	Ru	Re	Ta	W
{111}[11−2]	τ_{IS}	5.768	5.660	6.749	6.810	6.408	7.122	6.564	6.933
	γ_c	0.18	0.18	0.18	0.18	0.18	0.18	0.20	0.20
{111}[−110]	τ_{IS}	13.710	11.764	13.278	13.325	12.779	13.874	12.819	13.568
	γ_c	0.30	0.24	0.24	0.24	0.24	0.24	0.24	0.26

also interesting to notice that, under the {111}[11−2] slip systems, the corresponding critical shear strain, γ_c, is 0.18 for the alloying elements Re, Mo, Cr, Ru and Co, but it increases from 0.18 to 0.20 when doped with W and Ta, as shown in Table 1. For the {111}[−110] slip system, the addition of Re improves the ISS of the γ'-Ni_3Al phase, which is consistent with the previous results,[15] while the addition of the other alloying elements decreases the ISS of the system at 0 K, as visualized in Fig. 2(b). As shown in Table 1, the order of the ISS value is Re > undoped > W > Mo > Cr > Ta > Ru > Co. Furthermore, the γ_c of the pure Ni_3Al is 0.30, the γ_c of the system doped with W is 0.26, and the γ_c doped with the other alloying elements yield at the smaller strain of 0.24 at 0 K. The variation probably has something to do with charge redistribution and the bonding nature of X (X = Re, Ru, Ta, W, Mo, Cr, and Co) in the metallic compound, which will be discussed in the following section in terms of the density of states (DOS).

Fig. 3(a) and (b) plot the ISS values of the γ'-Ni_3Al doped with alloying elements as a function of temperature under the {111}[11−2] and{111}[−110] slip systems, respectively, where we can find a decreasing trend of the ISS with increasing temperature. This is consistent with the general observation for the material, wherein larger volumes (*e.g.*, at high temperature) cause weaker bonding strengths that lead to the decrease of the ISS. This is also in good agreement with previous predictions.[27] As shown in Fig. 3(a), when the temperature increases, the influences of the alloying elements upon the ISS of the {111}[11−2] slip system are consistent with the results at 0 K. That is to say, for the {111}[11−2] slip system, alloying does not considerably change the temperature dependence of the ISS, and Re, W and Mo at Al sites are the most effective elements for the strengthening the γ'-Ni_3Al phase. For the ISS of the {111}[−110] slip system in Fig. 3(b), however, careful observation shows that the addition of Re increases τ_{IS} as the temperature increases for the whole considered temperature range. Doping with W, the ISS value is less than that of the pure Ni_3Al at $T < 800$ K and greater than that of the pure Ni_3Al at $T > 800$ K. Namely, W has a discernible high-temperature relative strengthening effect against the {111}[−110] slip in the γ'-Ni_3Al phase. The rate of decrease of the ISS as a function of temperature for the γ'-Ni_3Al phase doped with

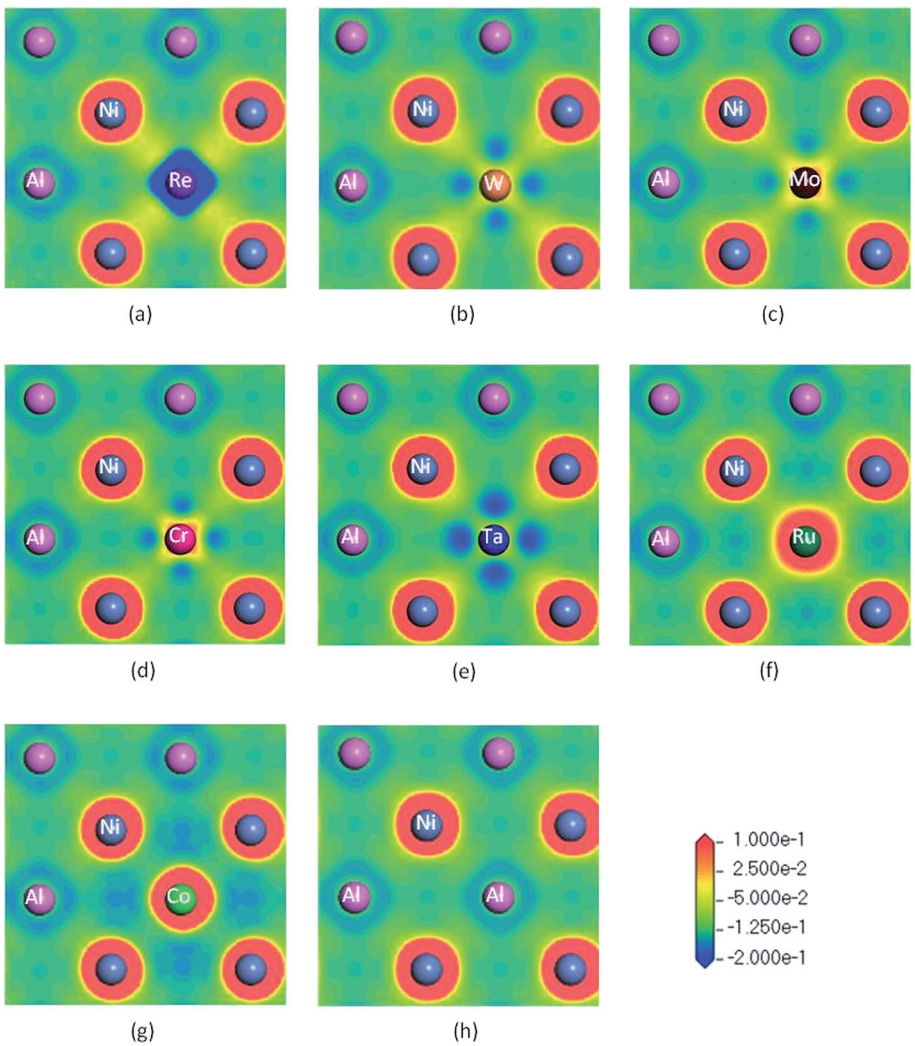

Fig. 4 Charge density difference of $Ni_{24}Al_7X$ (X = Re, W, Mo, Cr, Ta, Ru, Co, and Al) on the (100) plane. The different colors of the spheres represent the different elements. Note that, positive (negative) values denote the charge accumulation (depletion) in e (a.u.)$^{-3}$.

Mo gradually becomes small, so that the ISS of the Mo-doped γ'-Ni_3Al phase will be very close to the ISS of the W-doped and undoped γ'-Ni_3Al phase at high temperature. The effect of W and Mo upon the shear strength at high temperature is partially because alloying modulates the linear coefficients of thermal expansion.[27]

From the above discussion of the ISS, it can be found that the addition of almost all alloying elements can effectively suppress the shear deformation of the γ'-Ni_3Al phases. The effects of alloying with Re, W and Mo are the most obvious, especially at high temperature, which is consistent with the prediction that Re, W and Mo are important alloying elements for strengthening the Ni-based superalloys.[1]

3.2 Electronic structure

To understand the electronic basis of the shear strengthening of the γ'-Ni_3Al phase *via* alloying, we analyzed the charge density difference (CDD) and the total electronic density of states (TDOS) of the γ'-Ni_3Al phase. The CDD of $Ni_{24}Al_7X$ (X = Re, W, Mo, Cr, Ta, Ru, Co, and Al) on the (100) plane at zero strain are shown in Fig. 4, where an obvious directional distribution between X (Re, W, Mo, Cr and Ta) and their first nearest neighbor (1NN) Ni is observed. This indicates that the dopants Re (W, Mo, Cr and Ta) form covalent-like bonding with the 1NN Ni atoms, resulting in larger shear strength. The Co atom appears to form a typical metallic-like bonding with the 1NN Ni atom because the charge accumulation around Co is nearly spherically symmetric. As a result, shear softening is observed in the $Ni_{24}Al_7Co$ alloy. For Ru atom, the charge density between Ru and 1NN Ni atom almost spherical symmetric and a weak directional distribution is observed. In line with those discussed above, a small shear strengthening *via* Ru doping is observed in self consistent shear strength calculation.

For the {111}[11−2] and {111}[−110] slip systems, the TDOS of $Ni_{24}Al_7X$ (X = Al, Re, W, Mo, Cr, Ta, Ru, and Co) alloys at 0 K during the shear deformation are respectively pictured in Fig. 5

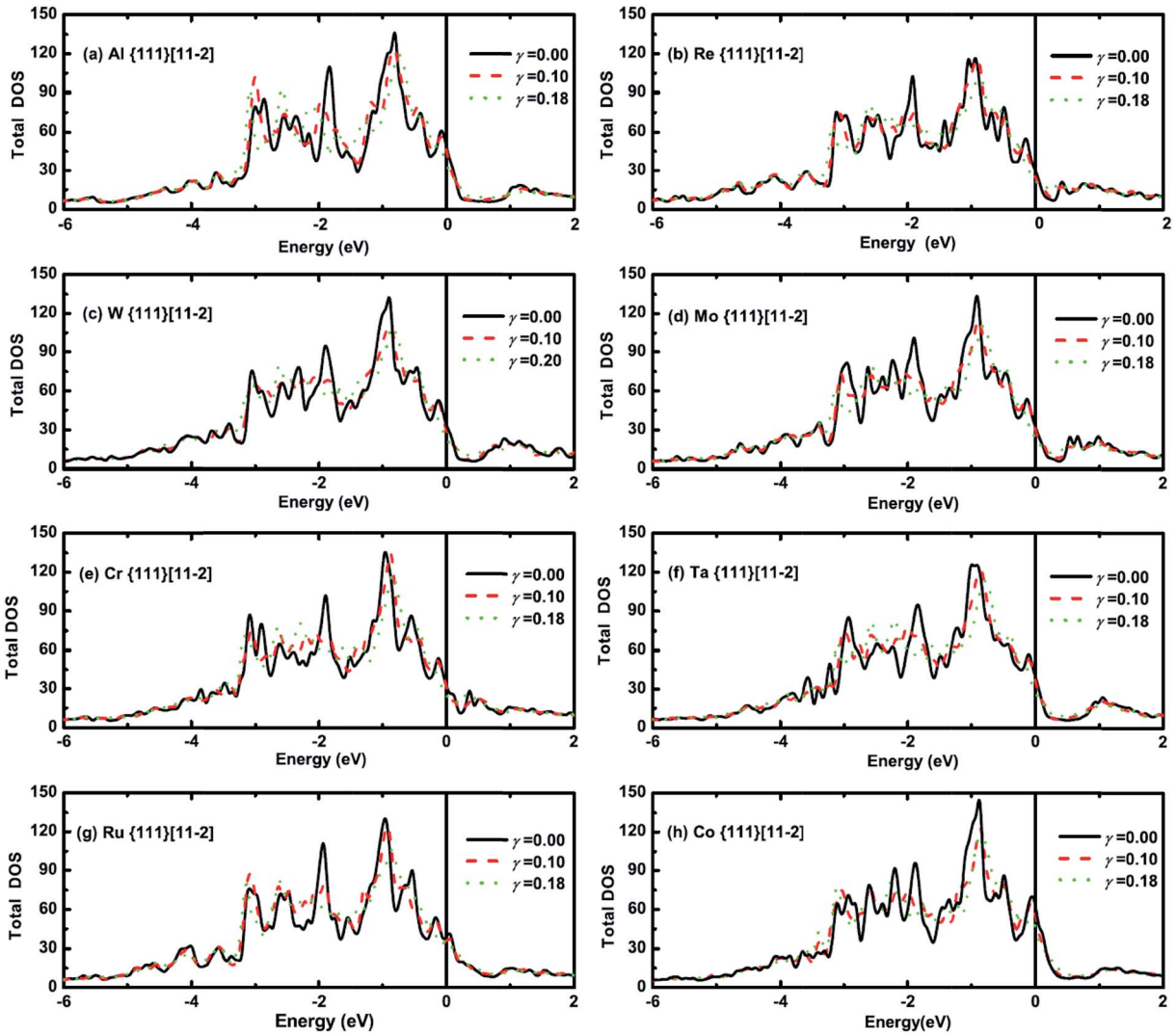

Fig. 5 Total electronic DOS of $Ni_{24}Al_7X$ alloys of the {111}[11−2] slip system with X = Al (a), Re (b), W (c), Mo (d), Cr (e), Ta (f), Ru (g) and Co (h) at different shear strains. The Fermi level is shifted to zero.

and 6. Comparing Fig. 5(a)–(h), one can find that the overall shape of the DOS changes marginally at the initial stage (γ = 0.00) for different alloying elements substituted into the Al site, but the energy band moves towards lower energies. For the ternary alloys with Re and W, particularly, the DOS peak just below the Fermi level moves noticeably to lower energies, which leads to a decrease in the electronic states at the Fermi level, as shown in Fig. 5(c) and (d). This fact demonstrates that the addition of these alloying elements can stabilize the system against lattice distortion, which is consistent with the CDD analysis. As can be seen from Fig. 5 for the {111}[11−2] slip system, the γ'-Ni_3Al phase has two pronounced DOS peaks at about −1 and −2 eV at zero strain. Upon shearing, these two peaks decrease gradually, indicating that the cubic symmetry of the system breaks and causes the DOS to become smooth, which leads to instability of the sheared γ'-Ni_3Al structure.

Fig. 6 shows the TDOS with the {111}[−110] slip system at 0 K for the different alloying elements during the shearing process. It is found that the change of DOS upon shearing along the [−110] direction exhibits different features from that along the [11−2] direction. For the [−110] direction, the DOS peaks located near −1 eV still gradually decrease and move towards higher energies, while the peaks near −2 eV almost disappear. More importantly, the pseudogap at ~0.4 eV becomes filled up during the shear deformation. When comparing the two slip systems, this filling up of the pseudogap is more sensitive to the {111}[−110] slip. For instance, the pseudogap is almost filled up at a shear strain of γ = 0.16 of the {111}[−110] slip, while a shoulder still remains at the pseudogap position for the {111}[11−2] slip systems with γ_c = 0.18. Therefore, we can conclude that total energy change should more sensitive to the {111}[−110] slip than the {111}[11−2] slip, which is to say that the

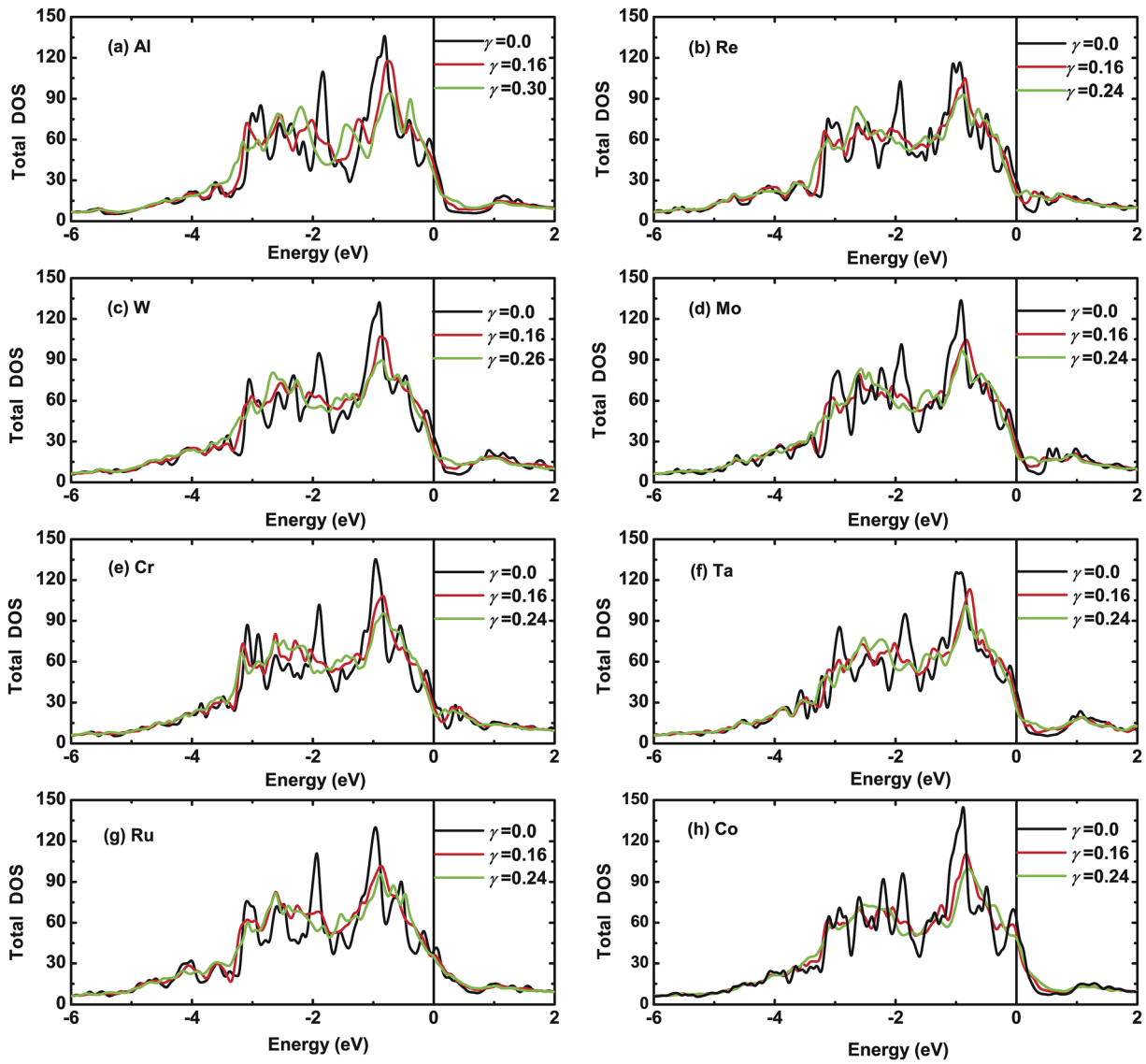

Fig. 6 Total electronic DOS of $Ni_{24}Al_7X$ alloys of the {111}[−110] slip system with X = Al (a), Re (b), W (c), Mo (d), Cr (e), Ta (f), Ru (g) and Co (h) at different shear strains. The Fermi level is shifted to zero.

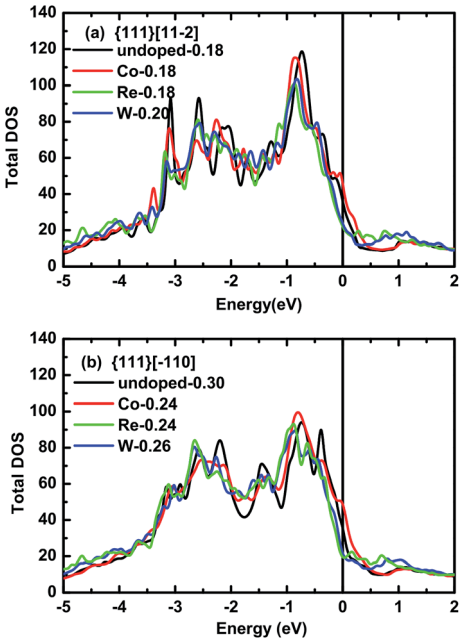

Fig. 7 Total electronic DOS of $Ni_{24}Al_7X_y$ alloys with X = Al, Co, Re, and W at the critical strain for (a) {111}[11−2] and (b) {111}[−110] slip systems. The Fermi level is shifted to zero.

{111}[11−2] system is the easy slip system and the {111}[−110] system is hard slip system.

To gain a deeper insight into the origin of the alloying effect, the total electronic DOS of $Ni_{24}Al_7X$ (X = Al, Co, Re, and W) alloys at the critical strain for the two slip systems are shown in Fig. 7. Compared with pure γ'-Ni_3Al, as shown in Fig. 7(a) ({111}[11−2] system), the Co-doped alloy possesses the largest spectral weights at the Fermi level. Contrarily, Re and W alloying decrease the DOS at the Fermi level and the Re-doped alloy has the smallest spectral weights at the Fermi level. Namely, the electronic DOS at the Fermi level experiences changes owing to alloying. According to the force theorem,[39,40] alloys with larger DOS at the Fermi level are more sensitive to shear deformation of the crystalline lattice.[41] Hence, the alloys that show a large DOS peak at the Fermi level (*e.g.*, $Ni_{24}Al_7Co$) should have smaller shear strengths. Conversely, the alloys with a small DOS peak or a DOS valley at the Fermi level will be less sensitive to deformation, and will thus have larger shear strengths. This simple scenario also covers the case of the {111}[−110] slip system (Fig. 7(b)), where the DOS of the Re-doped alloy is smallest at the Fermi level. Therefore, the ISS of the Re-doped alloy with the {111} plane along the [11−2] and [−110] direction is the largest among the doped γ'-Ni_3Al phase.

4. Conclusion

Using the first-principles approach in combination with the quasi-harmonic phonon approximation and the quasi-static approximation, we systematically investigate the influence of the alloying elements X (X = Re, Ru, Ta, W, Mo, Cr, and Co) upon the temperature-dependent ideal shear strength (ISS) τ_{IS} of the γ'-Ni_3Al phases for the two typical slip systems of {111}[11−2] and{111}[−110]. The results demonstrate that the ISS gradually decreases with increasing temperature and the alloying does not alter the temperature dependence of the ISS. Alloying considerably affects the ISS of the γ'-Ni_3Al phase at finite temperatures, however. For the {111}[11−2] slip systems, almost all of the alloying elements except for Co improve the ISS of the system at 0 K. Also, the corresponding critical shear strain γ_c is 0.18 with the addition of Re, Ru, Mo, Cr, and Co, which is identical to the γ_c of the pure Ni_3Al, but the γ_c value increases to 0.20 with the addition of W and Ta. Among the alloying elements, Re, W, and Mo are the most effective; but for the {111}[−110] slip systems, the addition of Re increases the ISS of Ni_3Al consistent with the previous studies, and the other alloying elements decrease the ISS of the system at 0 K. With increasing temperature, W strengthens the γ'-Ni_3Al phase at high temperature (T > 800 K), and the decreasing rate of the ISS as a function of temperature for the γ'-Ni_3Al phase doped with Mo gradually becomes small and thus the ISS of the Mo-doped γ'-Ni_3Al phase will be very close to the ISS of the W-doped and undoped γ'-Ni_3Al phase at high temperature. In comparison, the influences of the other alloying elements are identical with the strength at 0 K. The critical shear strain γ_c of {111}[−110] slip systems reduces from 0.30 to 0.24 at 0 K for almost all alloying elements except W, and γ_c of Ni_3(Al, W) is 0.26. Furthermore, analysis of the DOS of the Ni_3(Al, X) (X = Al, Re, W, and Co) systems during the process of shear deformation is also provided.

Acknowledgements

This work is supported by "973 Project" from the Ministry of Science and Technology of China (Grant No. 2011CB606402), the National Natural Science Foundation of China (Grant No. 51071091) and the Innovation Funds of Inner Mongolia University of Science and Technology (2010NC059). Simulations were performed using the "Explorer 100" cluster system at the Tsinghua National Laboratory for Information Science and Technology, Beijing, China.

References

1 R. C. Reed, *The Superalloys: Fundamentals and Applications*, Cambridge University Press, New York, 2006.
2 T. M. Pollock and S. Tin, *J. Propul. Power*, 2006, **22**, 361–374.
3 H. K. D. H. Bhadeshia, *Nickel Based Superalloys*, The website of University of Cambridge, http://www.msm.cam.ac.uk/phase-trans/2003/Superalloys/superalloys.html, accessed 12 November 2015.
4 M. Jahnatek, J. Hafner and M. Krajci, *Phys. Rev. B: Condens. Matter Mater. Phys.*, 2009, **79**, 224103.
5 Q. Feng, T. K. Nandy, S. Tin and T. M. Pollock, *Acta Mater.*, 2003, **51**, 269.
6 X. X. Yu, C. Y. Wang, X. N. Zhang, P. Yan and Z. Zhang, *J. Alloys Compd.*, 2014, **582**, 299.
7 S. Y. Wang, C. Y. Wang, J. H. Sun, W. H. Duan and D. L. Zhao, *Phys. Rev. B: Condens. Matter Mater. Phys.*, 2001, **65**, 035101.

8 Y. Zhou, Z. G. Mao, C. Booth-Morrison and D. N. Seidman, *Appl. Phys. Lett.*, 2008, **93**, 171905.
9 D. Lorenz, A. Zeckzer, U. Hilpert, P. Grau, H. Johansen and H. S. Leipner, *Phys. Rev. B: Condens. Matter Mater. Phys.*, 2003, **67**, 172101.
10 A. Kelly and N. H. Macmillan, *Strong Solids*, Clarendon Press, Oxford, 1986.
11 X. Q. Li, S. Schönecker, J. J. Zhao, B. Johansson and L. Vitos, *Phys. Rev. B: Condens. Matter Mater. Phys.*, 2013, **87**, 214203.
12 D. Roundy, C. R. Krenn, M. L. Cohen and J. W. Morris Jr, *Phys. Rev. Lett.*, 1999, **82**, 2713.
13 L. L. Yue, Y. Zhang, H. B. Zhou, G. H. Lu and M. Kohyama, *J. Phys.: Condens. Matter*, 2008, **20**, 335216.
14 M. Šob, L. G. Wang and V. Vitek, *Mater. Sci. Eng., A*, 1997, **1075**, 234.
15 Y. J. Wang and C. Y. Wang, *Scr. Mater.*, 2009, **61**, 197–200.
16 Y. J. Wang and C. Y. Wang, *Appl. Phys. Lett.*, 2009, **94**, 261909.
17 M. Kohyama, *Phys. Rev. B: Condens. Matter Mater. Phys.*, 2002, **65**, 184107.
18 G. H. Lu, Y. Zhang, S. H. Deng, T. M. Wang, M. Kohyama, R. Yamamoto, F. Liu, K. Horikawa and M. Kanno, *Phys. Rev. B: Condens. Matter Mater. Phys.*, 2006, **73**, 224115.
19 Y. Zhang, G. H. Lu, S. H. Deng, T. M. Wang, H. B. Xu, M. Kohyama and R. Yamamoto, *Phys. Rev. B: Condens. Matter Mater. Phys.*, 2004, **75**, 174101.
20 A. M. Iskandarov, S. V. Dmitriev and Y. Umeno, *Phys. Rev. B: Condens. Matter Mater. Phys.*, 2011, **84**, 224118.
21 W. Zhou, Y. Zhang, H. Sun and C. F. Chen, *Phys. Rev. B: Condens. Matter Mater. Phys.*, 2012, **86**, 054118.
22 S. L. Shang, W. Y. Wang, Y. Wang, Y. Du, J. X. Zhang, A. D. Patel and Z. K. Liu, *J. Phys.: Condens. Matter*, 2012, **24**, 155402.
23 K. Durst and M. Göken, *Mater. Sci. Eng., A*, 2004, **387**, 312.
24 S. L. Shang, D. E. Kim, C. L. Zacherl, Y. Wang, Y. Du and Z. K. Liu, *J. Appl. Phys.*, 2012, **112**, 053515.
25 Y. Wang, J. J. Wang, H. Zhang, V. R. Manga, S. L. Shang, L. Q. Chen and Z. K. Liu, *J. Phys.: Condens. Matter*, 2010, **22**, 225404.
26 R. Wang, S. F. Wang, X. Z. Wu and Y. Yao, *Phys. B*, 2011, **406**, 3951.
27 X. X. Wu and C. Y. Wang, *J. Phys.: Condens. Matter*, 2015, **27**, 295401.
28 F. D. Murnaghan, *Proc. Natl. Acad. Sci. U. S. A.*, 1944, **30**, 244.
29 S. L. Shang, W. Y. Wang, Y. Wang, Y. Du, J. X. Zhang, A. D. Patel and Z. K. Liu, *J. Phys.: Condens. Matter*, 2012, **24**, 155402.
30 F. R. De Boer, C. J. Schinkel, J. Biesterbos and S. Proost, *J. Appl. Phys.*, 1969, **40**, 1049.
31 P. E. Blöchl, *Phys. Rev. B: Condens. Matter Mater. Phys.*, 1994, **50**, 17953.
32 G. Kresse and D. Joubert, *Phys. Rev. B: Condens. Matter Mater. Phys.*, 1999, **59**, 1758.
33 G. Kresse, M. Marsman and J. Furthmüller, *VASP manual*, http://cms.mpi.univie.ac.at/vasp/vasp/vasp.html.
34 J. P. Perdew, K. Burke and M. Ernzerhof, *Phys. Rev. Lett.*, 1996, **77**, 3865.
35 H. J. Monkhorst and J. D. Pack, *Phys. Rev. B: Condens. Matter Mater. Phys.*, 1976, **13**, 5188.
36 M. Methfessel and A. T. Paxton, *Phys. Rev. B: Condens. Matter Mater. Phys.*, 1989, **40**, 3616.
37 A. van de Walle, M. Asta and G. Ceder, *Comput. Coupling Phase Diagrams Thermochem.*, 2002, **26**, 539.
38 A. Togo, F. Oba and I. Tanaka, *Phys. Rev. B: Condens. Matter Mater. Phys.*, 2008, **78**, 134106.
39 H. L. Skriver, *Phys. Rev. B: Condens. Matter Mater. Phys.*, 1985, **31**, 1909.
40 A. R. Mackintosh and O. K. Andersen, *Electrons at the Fermi Surface*, Cambridge University Press, Cambridge, 1980.
41 H. L. Zhang, M. P. J. Punkkinen, B. Johansson, S. Hertzman and L. Vitos, *Phys. Rev. B: Condens. Matter Mater. Phys.*, 2010, **81**, 184105.